

IMPROVING OBJECT DETECTION AND ATTRIBUTE RECOGNITION BY FEATURE ENTANGLEMENT REDUCTION

Zhaoheng Zheng, Arka Sadhu and Ram Nevatia*

University of Southern California
Los Angeles, USA

ABSTRACT

We explore object detection with two attributes: color and material. The task aims to simultaneously detect objects and infer their color and material. A straight-forward approach is to add attribute heads at the very end of a usual object detection pipeline. However, we observe that the two goals are in conflict: Object detection should be attribute-independent and attributes be largely object-independent. Features computed by a standard detection network entangle the category and attribute features; we disentangle them by the use of a two-stream model where the category and attribute features are computed independently but the classification heads share Regions of Interest (ROIs). Compared with a traditional single-stream model, our model shows significant improvements over VG-20, a subset of Visual Genome, on both supervised and attribute transfer tasks.

Index Terms— Object Detection, Attribute Recognition

1. INTRODUCTION

Object detection has seen tremendous progress through deep neural networks [1, 2, 3, 4, 5, 6] and availability of large scale datasets such as MS-COCO [7] and Visual Genome [8]. In addition to objects, attributes are useful in distinguishing among members of the same category. While attribute recognition is a classic topic when applied to homogeneous patches, the task is much more complex when applied to an entire object. Recently, joint prediction of objects and attributes has been explored under scene-graph generation [9], symbolic VQA [10], dense captioning [11] and image captioning [12]. In particular, the model used in [12] has been widely adopted as the feature extractor for VQA tasks, and as such forms a competitive baseline in our experiments. However, prior work does not evaluate performance on novel object-attribute pairs; in this paper, we explore the usual object-attribute detection problem and extension to recognition of novel object-attribute pairs.

In Fig. 1, we show some examples of objects with color attributes. Note that the “red car” can be distinguished from

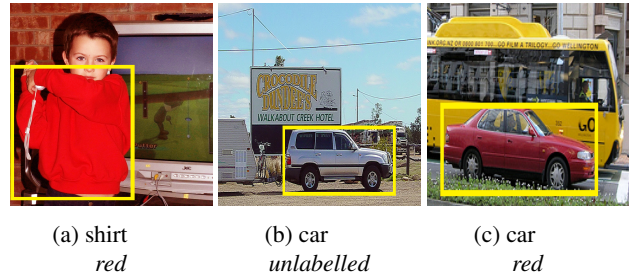


Fig. 1: Attribute Transfer: During training phase, some categories *e.g.* (a) come with attribute labels, while some *e.g.* (b) only have object class labelled. Models need to recognize attributes on such *unlabelled* categories, *e.g.* (c) during testing.

a “silver car” based on color. We note that the property of color is not specific to the car. Unlike naming color on patches [13, 14], recognizing the color of an object is more challenging. Typical objects are not of a single, uniform hue with further variations due to changes in surface orientation, illumination, reflections, shadows, and highlights. The material composition may also not be uniform; for example, a car has both metal and glass components. One other difficulty is created with the use of rectangular bounding boxes for object proposals which mix background pixels with object pixels. We do not aim to separate these influences; instead, as in object classification, we aim to learn from examples where the variations are accounted for in a holistic feature vector.

A further challenge is that common detection datasets do not come with attribute annotations; even in those, such as Visual Genome [8], that do provide attributes, a large proportion of objects is not attribute annotated. Additionally, as shown in Fig. 1, it is not reasonable to expect training data to contain all possible attribute-category pairs; a desirable model needs to recognize novel attribute-category pairs not encountered in training, we name this task as one of attribute transfer.

There is an inherent conflict between the feature requirements of category and attribute classification tasks: the former aims to be largely attribute-invariant and the latter to be largely invariant to category class. Simply attribute classification heads to the end of a two-stage detection pipeline (for

*This material is based upon work supported by the Defense Advanced Research Projects Agency (DARPA) under Agreement No. HR00111990059.

instance, Faster R-CNN [1]) entangles the features for two conflicting needs, weighing on the performance of both object detection and attribute prediction.

To eliminate potential entanglement in feature space, we separate the feature extraction into two streams. More specifically, in our proposed model, category classifier and attribute classifier are fed with separate features from two independent convolutional backbones, while region proposals are shared.

We evaluate the accuracy of single-stream and two-stream variants on VG-20, which we construct from the Visual Genome [8] dataset. We further construct novel splits from these datasets and investigate the ability of the models to transfer attributes. Our experiments show that in a single-stream architecture, incorporating attribute heads results in a significant drop in object detection mAP whereas there is little or no loss in the two-stream variants under novel attribute-category combinations and that the two-stream architecture achieves higher attribute transfer accuracy.

Our contributions are: (i) we eliminate the feature entanglement and resolve the internal conflict between object detection and attribute classification through the two-stream design; (ii) VG-20, a new subset of Visual Genome and splits in this dataset for evaluating attribute inference and transfer performance; (iii) demonstration of significant improvements over baselines for attribute inference and transfer tasks.

2. METHOD

R-CNN Detection Structure: Recent detection structures in the R-CNN family are composed of four parts: a deep convolutional backbones like ResNet [15] and VGG [16], the Region Proposal Network (RPN) [1], a feature extractor and a classification module. Specifically, the convolutional backbone processes image-level features from input images, and the RPN, takes features to generate proposals, or in other words, RoIs. The RoI feature extractor extracts features for these regions of interest via RoI Pooling operations. The classification module uses these RoI features to classify and regress the bounding box. In our case, we additionally have an attribute head for attribute classification.

Attribute Recognition with Object Embedding: Anderson *et al.* [12] introduced an additional substructure designed for attribute recognition. An embedding layer maps object labels into features, which are concatenated with RoI features, followed by a linear layer and finally fed to the classification heads for prediction. Such a structure brings object information to the attribute classification. But the conflict between object detection and attribute recognition remains.

Two-Stream Architecture: The proposed architecture follows the R-CNN pipeline, with the backbone and RoI feature extractor divided into two independent streams, as shown in Fig. 2. The object head and box head are kept in the object stream while the attribute stream makes attribute predictions. We choose to use the same stream for both color

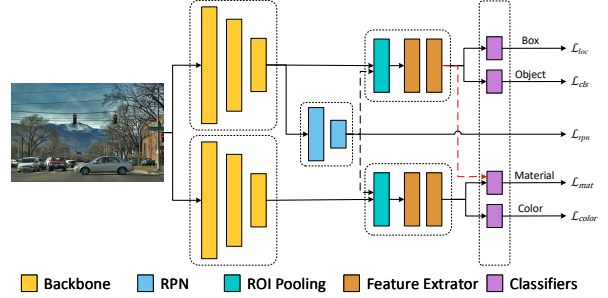


Fig. 2: Our two-stream architecture: Note that solid arrows are active in both inference and back propagation while dotted arrows are only active in inference.

and material attributes based on similar requirements of feature extraction. On top of the R-CNN pipeline, we add an attribute feature extractor which uses the RoI from RPN. The RPN is integrated into the object stream and takes features from the object backbone to generate region proposals. Region proposals are shared by both streams because attributes are properties associated with certain objects and computing proposals solely for attributes would be meaningless.

Cross Link: In the ordinary two-stream design, the object stream (the top side) and the attribute stream (the bottom side) make predictions from separate features computed by independent feature extractors. But unlike objects and color, objects and material are highly correlated. While some objects appear in some colors only, most man-made objects can appear in a variety of colors whereas the material property is much more constrained. To leverage such correlation, we add a cross link, the red dotted arrow in Fig. 2, from the object stream to the attribute stream. Features are concatenated before the prediction layer. Furthermore, the gradient from the material head to the object stream is blocked so that utilizing object features for attributes will not impair object detection.

Objectives: The overall loss function \mathcal{L} is the sum of four components $\mathcal{L}_{rpn}, \mathcal{L}_{loc}, \mathcal{L}_{cls}, \mathcal{L}_{attr}$, that is, $\mathcal{L} = \mathcal{L}_{rpn} + \mathcal{L}_{loc} + \mathcal{L}_{cls} + \mathcal{L}_{attr}$. In terms of \mathcal{L}_{loc} and \mathcal{L}_{cls} , we follow the same objective function proposed in [17]. As for \mathcal{L}_{rpn} , the loss function of RPN, we follow the one defined in [1]. And $\mathcal{L}_{attr} = \mathcal{L}_{color} + \mathcal{L}_{mat}$ Here,

$$\mathcal{L}_{color} = H(\sigma(\mathbf{z}_{color}), \mathbf{y}_{color}), \quad (1)$$

$$\mathcal{L}_{mat} = H(\sigma(\mathbf{z}_{mat}), \mathbf{y}_{mat}). \quad (2)$$

Note that H is the cross-entropy loss, σ refers to the softmax function, and \mathbf{z}, \mathbf{y} are inference scores and labels respectively. We name \mathcal{L}_{attr} as Separated Cross-Entropy loss (SCE) given that it is the sum of two independent cross-entropy functions.

Model	Object mAP @.5	Color Recall @.5	Material Recall @.5
PA + SCE	24.95	67.77	56.98
PA + UCE	25.35	68.74	56.01
Single-Stream (SS)	25.13	68.59	61.22
SS Detection Only	38.18	-	-
Two-Stream (TS)	38.17	72.40	63.83
TS + Cross Link	38.30	73.11	65.39
TS + LFE	28.37	72.72	63.50

Table 1: Results of Supervised Object Detection and Attribute Prediction: PA refers to the detection model used in [12]. LFE refers to the variation with Late Fusion Entanglement.

3. EXPERIMENTS

We introduce our data preparation in Sec. 3.1 and detail our experimental setup in Sec. 3.2, followed by quantitative results in Sec. 3.3 and qualitative visualizations in Sec. 3.4.

3.1. Data Preparation

To evaluate the performance of our approach, we construct a subset of Visual Genome [8]; specifically, we adopt the split and reorganized scene graphs created by Hudson *et al.* [18]. The Visual Genome dataset consists of 108k images along with over 1,600 object categories and around 400 attribute annotations associated with objects. However, many categories in the dataset overlap with other categories (for example, “man” and “person” are labeled as two different categories) and it also suffers from a long-tailed attribute distribution. Therefore, we pick 12 most descriptive colors and 4 most common materials from the dataset. Regarding object categories, we select 20 categories that have sufficient attribute annotations for our task. Thus we call our dataset as VG-20. In total, we have 180k samples for training and 25k for testing, with around one-third of them possess attribute annotations. Note that each bounding box is counted as one object sample and some bounding boxes do not have associated attribute annotations; we preserve these as they are useful in both training and evaluating object detectors.

3.2. Experimental Setup

We explore two settings w.r.t attribute annotations:

- **Supervised:** all attribute annotations are available during training phase.
- **Attribute Transfer:** objects are divided into two groups by their object labels, reference categories X_{ref} and target categories X_{tgt} . During training, objects in X_{ref} keep their attribute annotations while those in X_{tgt} do not have access to the attribute annotations. That is, the model needs to transfer attributes from X_{ref} to X_{tgt} which brings additional complexity.

	Model	Object mAP @.5	Color Recall @.5	Material Recall @.5
Target	PA + SCE	25.09	50.89	47.85
	PA + UCE	24.13	52.75	46.40
	Single-Stream	24.87	48.39	49.92
	Two-Stream (TS)	38.11	54.98	49.27
	TS + Cross Link	38.39	61.01	52.28
	TS + LFE	27.39	46.55	48.93
Reference	PA + SCE	23.27	67.26	59.70
	PA + UCE	22.32	66.41	58.62
	Single-Stream	22.76	67.39	61.48
	Two-Stream (TS)	37.67	69.43	62.67
	TS + Cross Link	38.26	71.73	66.14
	TS + LFE	26.11	68.91	63.25

Table 2: Results of Attribute Transfer: We use metrics object mAP, color recall, material recall, as defined in Sec. 3.2. SCE and UCE are loss functions defined in Eqn. 1, 2 and Eqn. 3. And PA refers to the detection model in [12].

For fair evaluation of attribute transfer over all categories, we divide the objects into two groups X_A and X_B , which satisfy following properties: $X_A \cap X_B = \emptyset$, $X_A \cup X_B = X_{all}$ and keep $|X_A|=|X_B|=10$. We let $X_{ref} = X_A$, $X_{tgt} = X_B$ in one run and vice versa in the other. Quantitative numbers are averaged over those two runs.

Evaluation Metrics: For object detection, we adopt the commonly used mean Average Precision (mAP@0.5). Furthermore, to measure both detection and recognition performances simultaneously, we define “attribute recall” (attribute could be color or material) as the ratio of objects whose bounding boxes and attributes are detected and recognized by the model to all objects with valid attribute annotations.

Baselines: We compare our model against two baseline approaches and one variation of our design.

- *Single-Stream:* A single-stream version of our model.
- *Peter Anderson Model (PA):* The R-CNN-like structure proposed in [12]. For fair comparison, we integrate an FPN to this model and retrain it with our data splits. The original PA model uses Unified Cross-Entropy loss:

$$\mathcal{L}_{attr} = H(\sigma(\mathbf{z}), \mathbf{y}), \quad (3)$$

where each color and material is treated as an attribute. We compare with two variants of PA, one trained with Unified Cross-Entropy (UCE) and the other with Separated Cross-Entropy (SCE), referred as PA + UCE and PA + SCE respectively.

- *Late Feature Entanglement (LFE):* A variation of our two-stream model where features from both streams are explicitly entangled. More specifically, RoI features from both streams are concatenated before classification so that all classifiers share identical features.

Implementation Details: We adopt ResNet-101 [15] as our backbones in both streams and the design of RPN follows

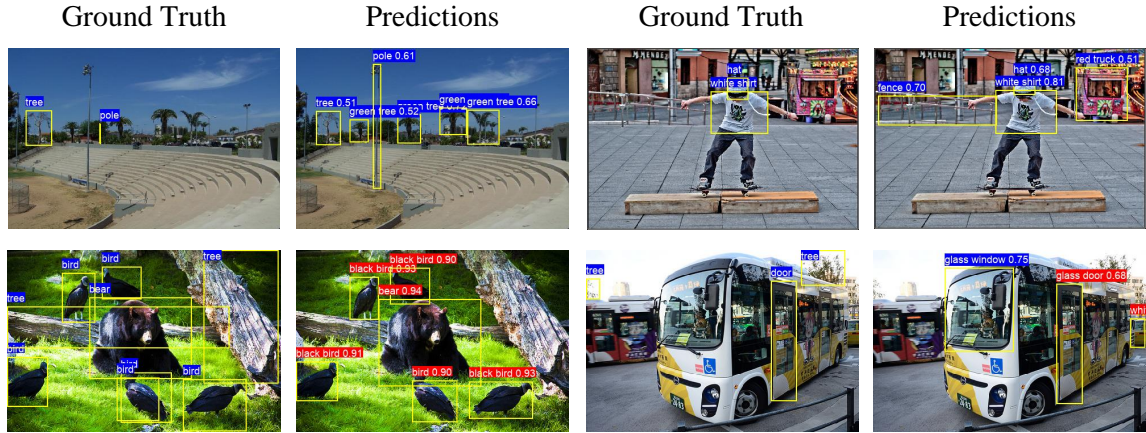


Fig. 3: Visualized detection results for VG-20 supervised (row 1), VG-20 attribute transfer (row 2). Object predictions colored in blue belong to reference set while those colored in red belong to target set in the attribute transfer setting.

[1]. We build the feature extractors following Feature Pyramid Networks (FPN) in [19]. During training, both streams of our model are initialized with the pre-trained weights from MSCOCO [7]. The model is trained by Adam [20] Optimizer with a learning rate of $5e - 5$. The batch size is set to 12.

3.3. Quantitative Results

We report results for VG-20 in both supervised and attribute transfer setting.

(a) **Supervised:** As seen in Table 1 for VG-20, compared with the detection only model, the single-stream detection plus attribute inference model brings down the object mAP by more than 10%. The two-stream variants do not exhibit this drop and also show a $\sim 3\%$ boost on color recall and an $\sim 2\%$ improvement on material recall. We also compare with our implementation of [12] with two different cross-entropy (PA + SCE and PA + UCE) which give similar results as single-stream models.

Furthermore, the late-stage feature entanglement does not show improvements in attribute recognition and even impairs the performance of object detection, dragging down object mAP by $\sim 10\%$. By comparing *Single-Stream* with *TS + LFE*, we demonstrate that, even though both object detection and attribute recognition benefit from the increased number of parameters, the feature entanglement between object stream and attribute stream leads to a significant deterioration on object-related performances.

(b) **Attribute Transfer:** Results on VG, shown in Tab. 2, also show noticeable improvements. In color domain, our models increase the performance by more than 10% on color recall. Finally, results on reference set are consistent with those in supervised setting as expected.

Effectiveness of the Cross Link: As shown in Tab. 2, the cross link improves the performance of our two-stream model especially in transferring attributes. The link improves the color recall and material recall in target categories by around 6% and 3%, respectively. Such results reflect that with less supervision, the cross link enables the attribute stream to learn from the object stream, resulting in the gain in attribute transfer.

3.4. Visualization

We visualize detection results of our two-stream model in Fig. 3 (only objects with confidence ≥ 0.5 are shown).

Supervised: Predictions are shown in first row. We note that the ground-truth annotations in VG are sparse (i) only some objects are annotated with bounding boxes (ii) even among objects with bounding boxes, only some are annotated with their color and material attributes. Though some objects are not annotated in the ground truth, our model provides reasonably dense predictions of objects and attributes.

Attribute Transfer: Examples in the second row show that our model can transfer attribute in real-world images. The colors of animals and materials of doors are well transferred.

4. CONCLUSION

We explore the task of jointly detecting objects and predicting their attributes. We show that naively attaching attribute heads to an R-CNN structure and jointly training object category and attribute leads to a significant drop in object detection performance due to feature entanglement. So we eliminate such feature entanglement via a two-stream pipeline with separate networks. We validate our approach on a subset of Visual Genome, VG-20. Experiments show that our method can effectively improve the performance on both tasks.

5. REFERENCES

- [1] Shaoqing Ren, Kaiming He, Ross Girshick, and Jian Sun, “Faster r-cnn: Towards real-time object detection with region proposal networks,” in *Advances in neural information processing systems*, 2015, pp. 91–99.
- [2] Kaiming He, Georgia Gkioxari, Piotr Dollár, and Ross Girshick, “Mask r-cnn,” in *Proceedings of the IEEE international conference on computer vision*, 2017, pp. 2961–2969.
- [3] Zhaowei Cai and Nuno Vasconcelos, “Cascade r-cnn: Delving into high quality object detection,” in *Proceedings of the IEEE conference on computer vision and pattern recognition*, 2018, pp. 6154–6162.
- [4] Jiangmiao Pang, Kai Chen, Jianping Shi, Huajun Feng, Wanli Ouyang, and Dahua Lin, “Libra r-cnn: Towards balanced learning for object detection,” in *Proceedings of the IEEE Conference on Computer Vision and Pattern Recognition*, 2019, pp. 821–830.
- [5] Jing Nie, Rao Muhammad Anwer, Hisham Cholakkal, Fahad Shahbaz Khan, Yanwei Pang, and Ling Shao, “Enriched feature guided refinement network for object detection,” in *The IEEE International Conference on Computer Vision (ICCV)*, October 2019.
- [6] Kaiwen Duan, Song Bai, Lingxi Xie, Honggang Qi, Qingming Huang, and Qi Tian, “Centernet: Keypoint triplets for object detection,” in *The IEEE International Conference on Computer Vision (ICCV)*, October 2019.
- [7] Tsung-Yi Lin, Michael Maire, Serge Belongie, James Hays, Pietro Perona, Deva Ramanan, Piotr Dollár, and C Lawrence Zitnick, “Microsoft coco: Common objects in context,” in *European conference on computer vision*. Springer, 2014, pp. 740–755.
- [8] Ranjay Krishna, Yuke Zhu, Oliver Groth, Justin Johnson, Kenji Hata, Joshua Kravitz, Stephanie Chen, Yanis Kalantidis, Li-Jia Li, David A Shamma, et al., “Visual genome: Connecting language and vision using crowdsourced dense image annotations,” *International Journal of Computer Vision*, vol. 123, no. 1, pp. 32–73, 2017.
- [9] Xiaodan Liang, Lisa Lee, and Eric P. Xing, “Deep variation-structured reinforcement learning for visual relationship and attribute detection,” *2017 IEEE Conference on Computer Vision and Pattern Recognition (CVPR)*, pp. 4408–4417, 2017.
- [10] Kexin Yi, Jiajun Wu, Chuang Gan, Antonio Torralba, Pushmeet Kohli, and Joshua B. Tenenbaum, “Neural-symbolic vqa: Disentangling reasoning from vision and language understanding,” in *Advances in Neural Information Processing Systems*, 2018, pp. 1039–1050.
- [11] Justin Johnson, Andrej Karpathy, and Li Fei-Fei, “Densecap: Fully convolutional localization networks for dense captioning,” in *Proceedings of the IEEE Conference on Computer Vision and Pattern Recognition*, 2016.
- [12] Peter Anderson, Xiaodong He, Chris Buehler, Damien Teney, Mark Johnson, Stephen Gould, and Lei Zhang, “Bottom-up and top-down attention for image captioning and visual question answering,” in *Proceedings of the IEEE conference on computer vision and pattern recognition*, 2018, pp. 6077–6086.
- [13] Xudong Han, Philip Schulz, and Trevor Cohn, “Grounding learning of modifier dynamics: An application to color naming,” in *Proceedings of the 2019 Conference on Empirical Methods in Natural Language Processing and the 9th International Joint Conference on Natural Language Processing (EMNLP-IJCNLP)*, 2019, pp. 1488–1493.
- [14] Olivia Winn and Smaranda Muresan, “‘lighter’ can still be dark: Modeling comparative color descriptions,” in *Proceedings of the 56th Annual Meeting of the Association for Computational Linguistics (Volume 2: Short Papers)*, 2018, pp. 790–795.
- [15] Kaiming He, Xiangyu Zhang, Shaoqing Ren, and Jian Sun, “Deep residual learning for image recognition,” in *Proceedings of the IEEE conference on computer vision and pattern recognition*, 2016, pp. 770–778.
- [16] Karen Simonyan and Andrew Zisserman, “Very deep convolutional networks for large-scale image recognition,” in *International Conference on Learning Representations*, 2015.
- [17] Ross Girshick, “Fast r-cnn,” in *Proceedings of the IEEE international conference on computer vision*, 2015, pp. 1440–1448.
- [18] Drew A Hudson and Christopher D Manning, “Gqa: A new dataset for real-world visual reasoning and compositional question answering,” *Conference on Computer Vision and Pattern Recognition (CVPR)*, 2019.
- [19] Tsung-Yi Lin, Piotr Dollár, Ross Girshick, Kaiming He, Bharath Hariharan, and Serge Belongie, “Feature pyramid networks for object detection,” in *Proceedings of the IEEE conference on computer vision and pattern recognition*, 2017, pp. 2117–2125.
- [20] Diederick P Kingma and Jimmy Ba, “Adam: A method for stochastic optimization,” in *International Conference on Learning Representations (ICLR)*, 2015.